Theoretical Study of Structure and Photophysics of Homologous Series of Bis(arylydene)cycloalkanones

Roman O. Starostin , Alexandra Ya. Freidzon * , Sergey P. Gromov

Posted Date: 21 July 2023

doi: 10.20944/preprints202307.1488.v1

Keywords: bis(arylydene)cycloalkanone dyes; photophysical properties; photochemical properties; absorption; luminescence; trans-cis isomerization; quantum chemistry; density functional theory; potential energy surface; conical intersection

Article

Theoretical Study of Structure and Photophysics of Homologous Series of Bis(arylydene)cycloalkanones

Roman Starostin [1,2], Alexandra Freidzon [3,4,*] and S.P. Gromov [1,2]

[1] FSRC "Crystallography and Photonics", Photochemistry Center of RAS, Russian Academy, of Sciences, Novatorov Str. 7A-1, Moscow 119421, Russian Federation; star.roman-96@yandex.ru
[2] Department of Chemistry, M. V. Lomonosov Moscow State University, Leninskie Gory 1-3, Moscow 119991, Russian Federation; spgromov@mail.ru
[3] Institute of Nanoengineering in Electronics, Spintronics and Photonics, National Research Nuclear University MEPhI, Kashirskoye Shosse, 31, 115409 Moscow, Russia; freidzon.sanya@gmail.com
[4] Faculty of Chemistry, Molecular Chemistry and Materials Science, Weizmann Institute of Science, 234 Herzl Street, POB 26, Rehovot 7610001 Israel
* Correspondence: freidzon.sanya@gmail.com

Abstract: Photophysical properties of a series of bis(arylydene)cycloalkanone dyes with various donor substituentns are studied by quantum chemistry. Their capacity for luminescence and nonradiative relaxation through *trans-cis* isomerization is related to their structure, in particular, to the donor capacity of the substituents and the degree of conjugation due to the central cycloalkanone moiety. It is shown that cyclohexanone central moiety introduces distortions and disrupts the conjugation, thus leading to a nonmonotonic change in their properties. The increasing donor capacity of the substituents causes increase in the HOMO energy (raise of the oxidation potential) and decrease in the HOMO-LUMO gap, which results in the red shift of the absorption spectra. The ability of the excited dye to relax through fluorescence or through *trans-cis* isomerization is governed by the height of the barrier between the Franck–Condon and S1-S0 conical intersection regions on the potential energy surface of the lowest π-π* excited state. This barrier also correlates with the donor capacity of the substituents and the degree of conjugation between the central and donor moieties. The calculated fluorescence and *trans-cis* isomerization rates are in good agreement with the observed fluorescence quantum yields.

Keywords: bis(arylydene)cycloalkanone dyes; photophysical properties; photochemical properties; absorption; luminescence; trans-cis isomerization; quantum chemistry; density functional theory; potential energy surface; conical intersection

1. Introduction

Bis(arylidene)cycloalkanones (Figure 1), also known as symmetric cross-conjugated dienones, ketocyanine dyes, or diarylidene ketone derivatives, are D-π-A-π-D dyes with interesting photochemistry and photophysics. The electrochemistry, photophysics and photochemistry of bis(arylidene)cycloalkanone series have been studied extensively [1–3]. The compounds were found to exhibit efficient *trans-cis* photoisomerization reactions. This property makes bis(arylidene)cycloalkanones useful in the development of photoresponsive materials and devices, such as molecular switches and optical data storage. Bis(arylidene)cycloalkanone compounds display solvatochromic properties [4–6] and can be applied, for example, for determining the polarity of a medium [7,8]. Bis(arylidene)cycloalkanones modified with ionophoric fragments [9–11] form a basis for photocontrolled supramolecular devices.

Bis(arylidene)cycloalkanone compounds were found to exhibit strong two-photon absorption properties, which could be useful for two-photon microscopy and photodynamic therapy [12,13]. The studies found that the photophysical properties of the compounds were dependent on the size of the alicyclic ring, with larger rings leading to lower fluorescence quantum yields and shorter excited-state lifetimes. [11]. Ref. [14] discusses the recent advances on benzylidene cyclopentanones as

Preprints (www.preprints.org) | NOT PEER-REVIEWED | Posted: 21 July 2023 doi:10.20944/preprints202307.1488.v1

photosensitizers for two-photon polymerization. The study focuses on the symmetrically substituted benzylidene cyclopentanones and their ability to initiate polymerization. In Ref. [15] discusses the molecular structure and vibrational spectra of 2,6-bis(benzylidene)cyclohexanone molecule. The paper presents the near-infrared Fourier transform (NIR-FT) Raman and Fourier transform infrared (FT-IR) spectra of 2,6-bis(benzylidene)cyclohexanone molecule along with the density functional calculations. Numerous papers [16,17] discuss the photoprocesses, kinetics, and photoproducts of bis(arylidene)cycloalkanones and their derivatives with electron-donating substituents. The studies analyze the spectral, luminescent, and time-resolved properties of the compounds and their derivatives.

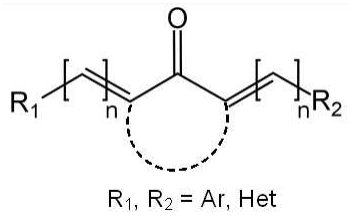

Figure 1. Schematic structure of ketocyanine dyes.

The electrochemistry and positions of the absorption and emission bands are immediately related to the electronic structure of the molecules in study, while the luminescence quantum yields and excitation decay kinetics are governed by the potential energy surfaces. The goal of this paper is to provide a quantum chemical interpretation of the photochemical and photophysical properties of the cycloalkanone series as a function of their molecular structure and important features of their potential energy surfaces. This study will help one gain deeper understanding of the structure–property relationships in bis(arylidene)cycloalkanone derivatives and facilitate their targeted molecular design.

2. Results

We consider a series of bis(benzylidene)cycloalkanone derivatives (Figure 2) with electron-donating groups in the phenyl rings. In polar solvents, such as acetonitrile, the global energy minimum corresponds to the sterically unhindered (*E,E*) isomers, while the gas phase structure, as predicted by the calculations, is (*Z,Z*) form stabilized by intramolecular C-H…O hydrogen bonds. Therefore, all the calculations were performed taking solvent into account within Polarizable Continuum Model.

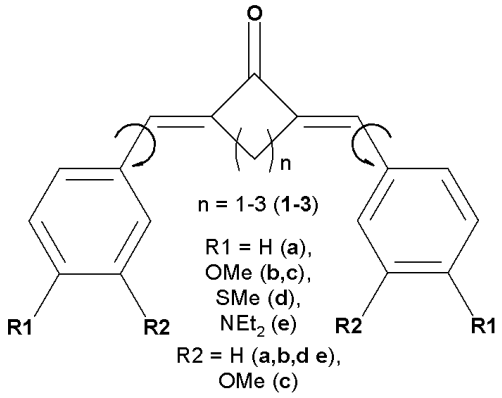

Figure 2. Dyes under study with important torsion angles shown by arrows.

Preprints (www.preprints.org) | NOT PEER-REVIEWED | Posted: 21 July 2023 doi:10.20944/preprints202307.1488.v1

2.1. Ground state structures and molecular orbitals

The calculations demonstrated that the fractions of (*E*,*Z*) and (*Z*,*Z*) isomers is negligible in the ground state. This agrees with the experiment [1–3,17], where no electronic transitions corresponding to (*E*,*Z*) and (*Z*,*Z*) isomers were observed in the absorption spectra. The ground-state rotation barriers are ~50-60 kcal/mol, which indicates that *trans-cis* isomerization in the ground state is impossible at any reasonable temperature.

The depths of the local minima associated with the rotation of the phenyl rings (shown by arrows in Figure 2) differ by a fraction of kilocalorie, and these minima are separated by low barriers, which can easily be overcome at room temperature, ensuring slightly hindered rotation of these groups. The 1H NMR experiments indicate that dyes **(1-3)c** exist as mixtures of rotamers [1–3].

The planarity of the molecule reflects the degree of conjugation in it. In bis(benzylidene)cycloalkanones under study the central part is rather rigid, but rotation is possible around formally single bonds shown in Figure 2 by arrows. Table 1 shows the corresponding torsion angles characterizing the effect caused by the central alicyclic fragment on the conjugated chromophore chain.

Table 1. Torsion angle (°) characterizing sterical distortion of π system.

	a	**b**	**c**	**d**	**e**
1	0.1	0.0	0.0	0.0	0.4
2	7.0	1.0	0.1	0.5	0.2
3	30.3	26.9	23.9	26.6	21.0

One can see that cyclobutanone central moiety favors perfectly conjugated chromophore chain, the distortion introduced by cyclopentanone is also minor, while that introduced by cyclohexanone is noticeable. Donor substituents favor the conjugation diminishing the torsion from 7° in **2a** to almost 0° in **2d,e**. The distortion caused by cyclohexanone is so large that even donor substituents reduce it from 30° in **3a** only to 21° in **3e**. The same trend is observed in the available crystal structures: 0-2° in cyclobutanones, 1-8° in cyclopentanones, and 9-39° in cyclohexanones.

The chemical shifts (Table S1 of Supplementary Materials) show the following trend with the increase of the central alicycle: the aliphatic protons shift towards strong fields, while methine protons shift towards weak fields. This trend is observed both in the calculated and experimental chemical shifts.

The donor capacity of the substituents is reflected by the Mulliken charges induced by the substituents on the phenyl rings (Table 2). In more conjugated systems, the electron density can flow freely from the donors to the acceptor, thus causing positive charge on the donors and negative on the acceptor. Due to the distorted conjugation, the electron density remains on the donors, and the charge on the donor fragment slightly decreases in cyclohexanone relative to cyclobutanone and cyclopentanone. As for the donor capacity of the substituents, the charges suggest the following order: 4-H < 4-OMe ~ 3,4-OMe ~ 4-SMe < 4-NEt2.

Table 2. Mulliken charges on donor fragments.

	a	**b**	**c**	**d**	**e**
1	0.11	0.14	0.14	0.13	0.20
2	0.10	0.13	0.12	0.11	0.19
3	0.07	0.10	0.10	0.09	0.16

Another way of characterizing donor capacity of the substituents is their effect on the frontier orbital energies, mainly, HOMO. Figure 3 shows that the trend observed in the Mulliken charges is pronounced more clearly in the HOMO energy: 4-H < 4-OMe < 3,4-OMe ~ 4-SMe < 4-NEt2. The LUMO

Preprints (www.preprints.org) | NOT PEER-REVIEWED | Posted: 21 July 2023 doi:10.20944/preprints202307.1488.v1

energy is mostly affected by the acceptor fragment, but the effect is much less pronounced. The HOMO-LUMO gap, which correlates with the absorption spectra, decreases in the series: 4-H > 4-OMe > 3,4-OMe ~ 4-SMe > 4-NEt2.

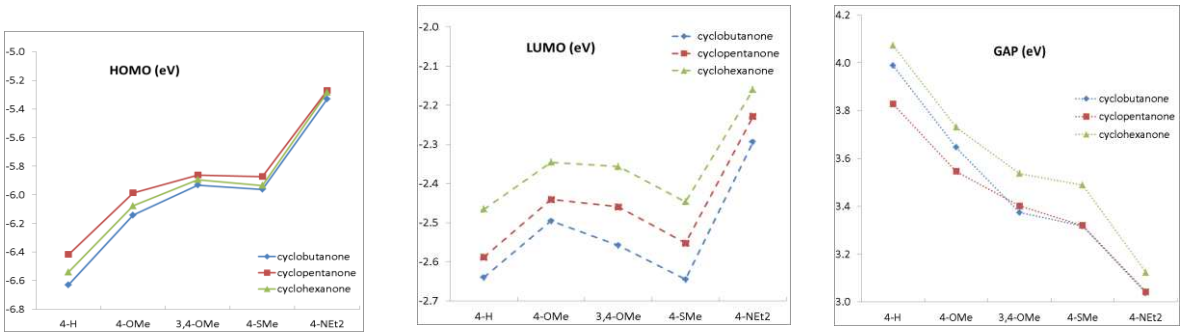

(**a**) (**b**) (**c**)

Figure 3. (a) HOMO, (b) LUMO energies and (c) HOMO-LUMO gap as functions of the donor substituents.

The HOMO-LUMO gap in cyclohexanone derivatives is in general higher than that in cyclobutanones and cyclopentanones owing to the distorted conjugation caused by the cyclohexanone moiety. This results in the blue-shifted spectra of the cyclohexanone derivatives. The HOMO and LUMO energies correlate with the oxidation and reduction potentials [1–3]. The HOMO-LUMO gaps also correlate with the experimental E_{ox}-E_{red} gaps (see Figures S2 and S3 of Supplementary materials).

2.2. Absorption and emission spectra

The most interesting properties of bis(benzylidene)cycloalkanones are their absorption and emission spectra and their phototransformations. In this section we consider the energy of the lowest π-π* electronic transition as a function of the donor capacity of the substituent and the size of the central alicycle (see Table S2 of Supplementary Materials).

The trends in the energy of the lowest π-π* electronic transition (Figure 4) resemble those of the HOMO-LUMO gap, because these transitions are mainly contributed by HOMO->LUMO excitation. As before, cyclohexanone dyes have higher excitation energies due to the distorted conjugation.

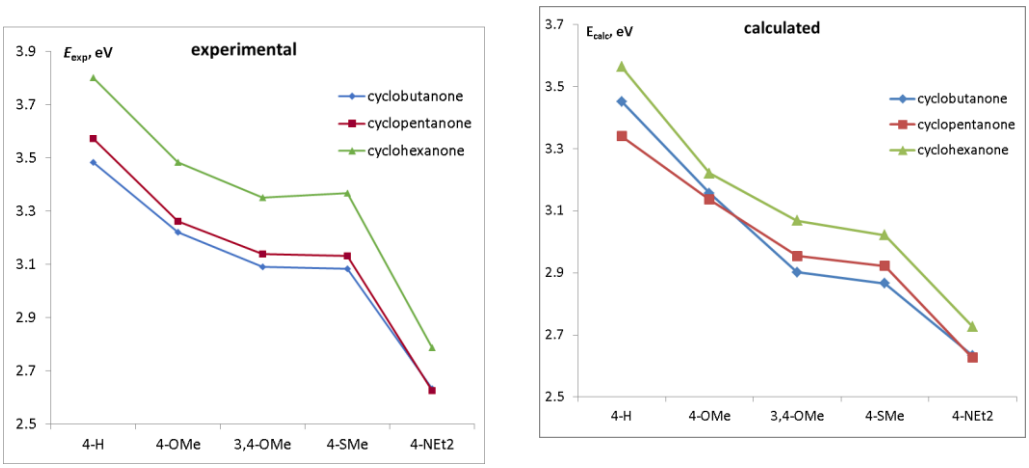

(**a**) (**b**)

Figure 4. (a) Experimental and (b) calculated energy of the lowest π-π* electronic transition as a function of the donor substituent.

Preprints (www.preprints.org) | NOT PEER-REVIEWED | Posted: 21 July 2023 doi:10.20944/preprints202307.1488.v1

Our calculations show that in addition to the intense π-π* and dark n-π* electronic transitions, the dyes exhibit one more π-π* electronic transition at ~400 nm resulting from HOMO-1->LUMO transition (Figure 5). The intensity of this transition decreases from cyclobutanone to cyclohexanone (Figure S4 of Supplementary Materials). This is supported by the experimental data [1–3,18,19]: in cyclobutanone **1e** the long-wave absorption band consists of two distinct peaks that cannot be attributed to the vibronic progression, while in **2e** and **3e** the long-wave absorption band is only broadened. The position of this band changes only slightly, which can be explained by the fact that HOMO-1 is not affected either by the substituents or by the central moiety.

The trends in the order of excited states are shown in Figure S5 of Supplementary Materials. The nπ* state is the lowest in the unsubstituted dyes **(1-3)a**, and goes up as soon as donor substituents appear in the *para* position. At the same time, the two ππ* states go down. In **(1-3)b**, the nπ* state lies between the two ππ* states. In the dyes with more donor substituents, the order of stated depends on the central alicycle: in the most conjugated **1(c-e)**, the nπ* state lies above both ππ* states, while in the other cycloalkanones, the nπ* state goes above both ππ* states only in **(2,3)e**.

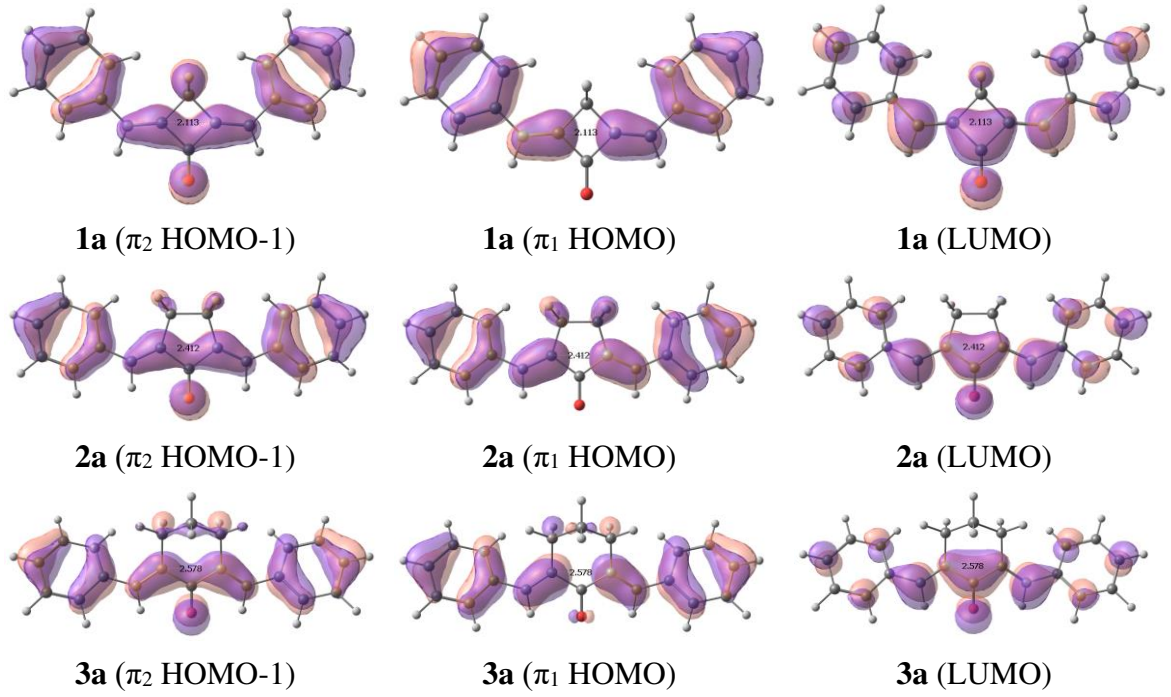

Figure 5. Frontier orbitals of **(1-3)a.**

Frequently the changes taking place in excited dyes, in particular, the bond length alternation in the excited state, which facilitates *trans-cis* isomerization, are explained in terms of resonance structures (see, for example, [20]). In most cases, these features are reflected by the nodal structure of HOMO and LUMO. The latter, being populated in the excited state, correlates with the resonance structure with alternated bonds. In the case of benzylidene cycloalkanones, the nodal structure of LUMO also corresponds to the resonance structure with alternated bonds. The bond length in the first ππ* excited state change in agreement with the nodal structure of LUMO: appearance of the node in LUMO as compared to HOMO results in bond lengthening, while disappearance of the node results in bond shortening. The change is noticeable, especially in the **(1-3)a**, up to 0.03-0.04 A. In general, the largest alternations are in the exocyclic double bonds and in the adjacent single bonds shown by arrows in Figure 2. In some cases, the carbonyl bond also changes.

All cyclobutanone dyes except for **1a** and **1b** are fluorescent, with the quantum yields increasing from **1c** to **1e**. Cyclopentanones **2c-e** are also fluorescent, while in cyclohexanones, only **3e** is fluorescent. For **(1-3)a**, the lack of luminescence can be explained by the fact that their first electronic transition is dark n-π*; therefore, excitation to the bright S2 (ππ*) only causes relaxation to the dark S1(nπ*), which further relaxes nonradiatively thorough internal conversion or intersystem crossing.

Preprints (www.preprints.org) | NOT PEER-REVIEWED | Posted: 21 July 2023 doi:10.20944/preprints202307.1488.v1

The lack of luminescence of other dyes, whose first electronic transition is bright π-π*, is more difficult to explain. To do this, one needs to consider the potential energy surfaces of the ground and first excited states or, more specifically, their cross-sections (profiles) along certain internal coordinates (Figure 6a).

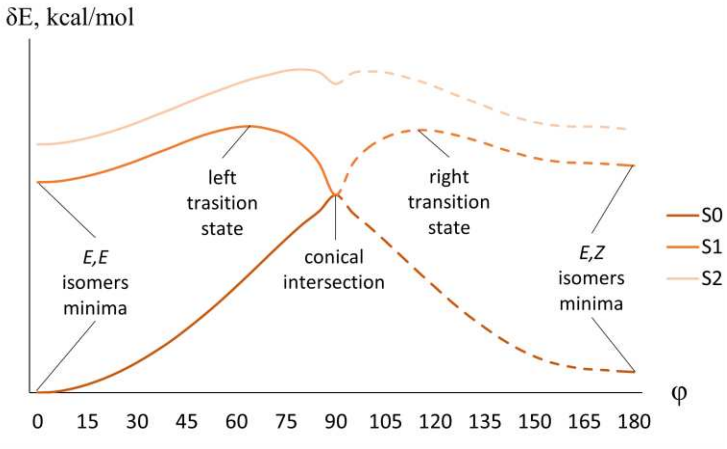

(a)

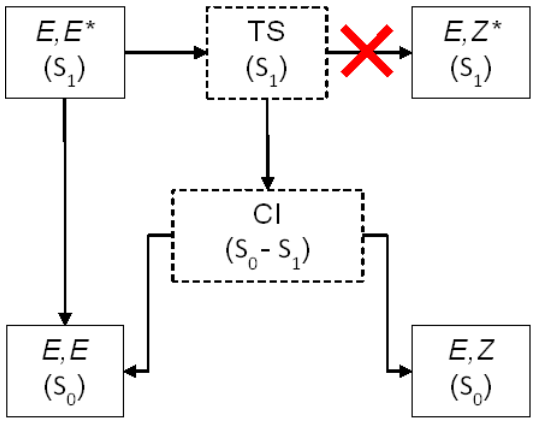

(b)

Figure 6. (a) Typical potential energy profile of the ground S0 and lowest excited S1 (ππ*) and S2 (nπ*) states. (b) Relaxation processes resulting in the *trans-cis* isomerization.

The internal coordinate involved in the relaxation of the S1 (ππ*) excited state of bis(arylidene)cycloalkanones is rotation along the formally double bond. This shape of the potential energy profile implies that the molecule excited from its global (*E*,*E*) minimum to the Franck-Condon region of the S1 state quickly relaxes to its nearest minimum. From this local minimum of the S1 state, the molecule can either emit light or further relax to the region of lower energy (here, it is the region of the S1-S0 conical intersection). If the barrier separating the local minimum from the CI region is not very high, this relaxation can successfully compete with the radiative relaxation. Near the CI point, the molecule quickly relaxes nonradiatively to the S0 state. From this point, the twisted chromophore can relax either back to the (*E*,*E*) region or forward to the (*E*,*Z*) region resulting in the *trans-cis* isomerization. Since the S1 state in the local minimum is rather short-lived (either owing to the radiative relaxation or to the structural relaxation to the CI), no equilibrium is possible on the S1 potential energy surface, and excited (*E*,*Z*)* states are not accessible directly from the excited (*E*,*E*)* states. All these processes are schematically shown in Figure 6b.

Preprints (www.preprints.org) | NOT PEER-REVIEWED | Posted: 21 July 2023 doi:10.20944/preprints202307.1488.v1

The right-hand part of the profile in Figure 6a represents the same process, but starting from the (*E,Z*) ground state structure. However, since the ground state is dominated by the (*E,E*) isomer, the right-hand part of the profile does not seem to be relevant.

Therefore, the luminescence quantum yield is governed by the competition between the radiative relaxation from the (*E,E*)* minimum and *trans-cis* photoisomerization. The triplet processes proceed on a microsecond timescale or even slower; therefore, we don't need to include them in the scheme.

Figure 7 shows the trends in the activation energy and CI depth as a function of donor substituents and central ring size. Although the CI depth cannot be a driving force for the *trans-cis* isomerization process, it is also indicative of the dye properties. the CI depth decreases and the activation energy increases with the increasing donor capacity of the substituent. The barrier height also increases from cyclohexanone to cyclobutanone. This is in line with the observed trend in the fluorescence quantum yields.

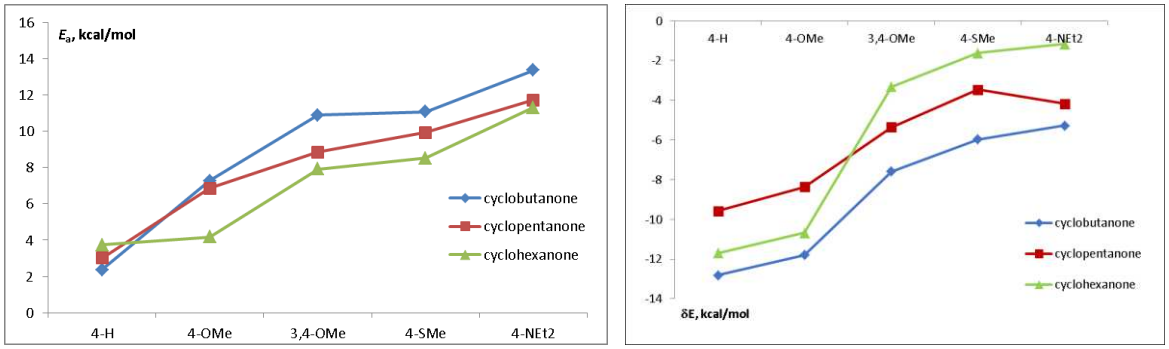

Figure 7. (a) The activation energy for the transition from *(E,E)* to CI and (b) CI depth in the S1 state.

Table 3 shows the radiative lifetimes calculated using the oscillator strengths of the S1-S0 transition, and characteristic *trans-cis* isomerization times calculated using the Arrhenius equation on the S1 potential energy surface of the *trans* isomer. One can see that emission can proceed in the nanosecond timescale, while *trans-cis* isomerization time can range from fractions of nanosecond to microseconds or longer. Fast isomerization successfully competes with the radiative decay channel, thus causing fluorescence quenching. One can see that *trans-cis* isomerization in **1(c-e)** is several orders of magnitude slower than in **1(a,b)**, and isomerization of **3b** competes with the radiative relaxation. In **3(c,d)**, relaxation *via* triplet state adds to the relaxation *via trans-cis* isomerization, The calculated *trans-cis* isomerization times correlate with the observed fluorescence of the cycloalkanones (Table S2 of Supplementary materials).

Table 3. Calculated radiative lifetime (τ_r) of *E,E* isomer of cycloalkanones, (*E,E*)-(*E,Z*) isomerization rate constant (k) and isomerization time (t_{tc}).

Cyclobutanone			
Dienone	τ_r, ns	k, s^{-1}	t_{tc}, ns
1a	-	$1.12 \cdot 10^{10}$	0.09
1b	2.28	$4.97 \cdot 10^{6}$	201
1c	3.05	$4.40 \cdot 10^{3}$	227400
1d	2.62	$4.06 \cdot 10^{3}$	2465000
1e	3.07	$1.22 \cdot 10^{2}$	8182600
Cyclopentanone			

Preprints (www.preprints.org) | NOT PEER-REVIEWED | Posted: 21 July 2023 doi:10.20944/preprints202307.1488.v1

2a	-	$4.66 \cdot 10^9$	0.21
2b	1.83	$8.28 \cdot 10^6$	121
2c	2.23	$8.13 \cdot 10^4$	12300
2d	1.97	$3.34 \cdot 10^4$	29900
2e	1.90	$2.55 \cdot 10^4$	39200
		Cyclohexanone	
3a	-	$1.41 \cdot 10^9$	0.71
3b	2.90	$5.47 \cdot 10^8$	1.83
3c	2.26	$7.12 \cdot 10^5$	1404
3d	2.02	$4.92 \cdot 10^5$	2033
3e	2.46	$3.40 \cdot 10^3$	294000

4. Materials and Methods

The structures and energies of the molecules were calculated using the density functional theory (DFT) with the PBE0 functional and 6-31+G(d,p) basis set by the FireFly program [21], partially based on GAMESS code [22]. The solvent (MeCN) effects were taken into account using the dielectric polarizable continuum model (D-PCM) [23]. Previously [10], we have shown that for dienones, solvent effects are important to properly reproduce the structures and conformation energies.

The vertical absorption and emission spectra, energy profiles of (*E,E*)-(*E,Z*) isomerization and rotation of the aromatic ring around C(β)-C(γ) bond were calculated by the time-dependent DFT (TDDFT) with the same functional, basis set, and solvent model. The vertical absorption spectra were calculated by the TDDFT after DFT optimization of the ground state geometry. A similar method was applied for vertical emission spectra calculations after geometry optimization of the π-π* lowest excited state using the TDDFT and D-PCM. The radiative lifetimes were calculated according to the formula:

$$k_r = (⅔) f_{0i} \nu^2_{i0};\ \tau_r = 1/k_r$$

where f_{0i} and ν_{0i} are oscillator strength and the frequency of the electronic transition of the ith isomer respectively; k_r is the radiation constant. The isomerization periods were calculated according to the formula:

$$k_{tc} = c\nu_i \cdot \exp(-E_{Ai}/RT);\ t_{tc} = 1/k_{tc}$$

where ν_i is the vibrational mode frequency of the *i*th isomer, and E_{Ai} is the activation barrier of this isomer.

The main channel of the structural relaxation of the S1 state of (*E,E*) bis(benzylidene)cycloalkanones is rotation around formally double bond leading to *trans-cis* isomerization. To construct the profiles of (*E,E*)-(*E,Z*) isomerization and an alternative channel, rotation of the aromatic ring around formally single bond, we used a simple (unrelaxed) scan of the potential energy surface along the corresponding dihedral angles. The energy values correspond to the non-optimized structures obtained by twisting of the initial isomer or rotamer. In the case of (*E,E*)-(*E,Z*) isomerization the left-hand rotation barriers were estimated by the energy difference of the maximum on the S1 profile (corresponding to the left transition state) and stable structures of the (*E,E*) isomers in the S1 state (left minimum).

We understand that phototransformation, which proceeds via a conical intersection, requires multireference quantum chemistry for an adequate description of the potential energy profiles [24].

Nevertheless, our semi-quantitative description gives insights into the mechanism of phototransformations in organic dyes [25].

The vertical ionization potentials (IP) and electron affinities (EA) were calculated by restricted-open-shell DFT (RO-DFT) for the corresponding monocation and monoanion of each dye. The functional, basis set, and solvation model were the same.

5. Conclusions

Photophysical properties of a series of bis(arylydene)cycloalkanone dyes with various donor substituentns are studied by quantum chemistry. Their capacity for luminescence and nonradiative relaxation through *trans-cis* isomerization is related to their structure, in particular, to the donor capacity of the substituents and the degree of conjugation due to the central cycloalkanone moiety. It is shown that cyclohexanone central moiety introduces distortions and disrupts the conjugation, thus leading to a nonmonotonic change in their properties. The donor capacity of the substituents is found to increase in the series 4-H < 4-OMe < 3,4-OMe ~ 4-SMe < 4-NEt2, which causes increase in the HOMO energy (raise of the oxidation potential) and decrease in the HOMO-LUMO gap (decrease in the excitation energy and a red shift of the absorption spectra). The ability of the excited dye to relax through fluorescence or through the *trans-cis* isomerization is governed by the height of the barrier between the Franck–Condon and S1-S0 conical intersection regions on the potential energy surface of the lowest π-π^* excited state. This barrier also correlates with the donor capacity of the substituents and the degree of conjugation between the central and donor moieties. The calculated fluorescence and *trans-cis* isomerization rates are in good agreement with the observed fluorescence quantum yields.

Supplementary Materials: The following supporting information can be downloaded at the website of this paper posted on Preprints.org, Figure S1: Calculated and experimental chemical shifts in 4-H, 4-OMe, and 3,4-OMe; Figure S2: Correlations between the calculated HOMO and LUMO energies and experimental oxidation and reduction potentials; Figure S3: Correlations between the calculated HOMO-LUMO gap and experimental gap between the oxidation and reduction potentials; Figure S4: Oscillator strengths of the first and second $\pi\pi^*$ transitions; Figure S5: Energy diagrams of the excited states of (E,E) isomer in cyclobutanone, cyclopentanone, and cyclopentanone series; Table S1: Comparison of experimental and calculated chemical shifts; Table S2: Experimental and calculated electronic transitions.

Author Contributions: Conceptualization, A.F.; methodology, A.F.; formal analysis, R.S.; investigation, A.F. and R.S.; writing—original draft preparation, A.F. and R.S.; writing—review and editing, A.F. and R.S.; visualization, A.F. and R.S.; supervision, S.G.; project administration, S.G.; funding acquisition, S.G. All authors have read and agreed to the published version of the manuscript.

Funding: This work was supported by the Russian Science Foundation (project No. 22-13-00064).

Data Availability Statement: The data presented in this study are available on request from the corresponding author.

Acknowledgments: The calculations were performed using the computational facilities of the Joint Supercomputer Center of the Russian Academy of Sciences.

Conflicts of Interest: The authors declare no conflict of interest. The funders had no role in the design of the study; in the collection, analyses, or interpretation of data; in the writing of the manuscript; or in the decision to publish the results.

References

1. Fomina, M.V.; Vatsadze, S.Z.; Freidzon, A.Y.; Kuz'mina, L.G.; Moiseeva, A.A.; Starostin, R.O.; Nuriev, V.N.; Gromov, S.P. Structure–Property Relationships of dibenzylidenecyclohexanones. *ACS Omega* **2022**, 7, 10087–10099.
2. Fomina, M.V.; Freidzon, A.Y.; Kuz'mina, L.G.; Moiseeva, A.A.; Starostin, R.O.; Kurchavov, N.A.; Nuriev, V.N.; Gromov, S.P. Synthesis, Structure and Photochemistry of Dibenzylidenecyclobutanones. *Molecules* **2022**, 27, 7602.
3. Vatsadze, S.Z.; Gavrilova, G.V.; Zyuz'kevich, F.S.; Nuriev, V.N.; Krut'ko, D.P.; Moiseeva, A.A.; Shumyantsev, A.V.; Vedernikov, A.I.; Churakov, A.V.; Kuz'mina, L.G.; et al. Synthesis, structure,

electrochemistry, and photophysics of 2,5- dibenzylidenecyclopentanones containing in benzene rings substituents different in polarity. *Russ. Chem. Bull*. **2016**, 65, 1761–1772.
4. Doroshenko, A.O.; Pivovarenko, V.G. Fluorescence quenching of the ketocyanine dyes in polar solvents: anti-TICT behavior, *J. Photochem. Photobiol. A*. **2003**, 156(1-3), 55–64,
5. Gutrov, V.N.; Zakharova, G.V.; Fomina, M.V.; Nuriev, V.N.; Gromov, S.P.; Chibisov, A.K. Molecular photonics of dienones based on cycloalkanones and their derivatives. *J. Photochem. Photobiol. A* **2022**, 425, 113678.
6. Homocianu, M.; Serbezeanu, D.; Tachita, V.B. Solvatochromism, Acidochromism and Photochromism of the 2,6-Bis(4-hydroxybenzylidene) Cyclohexanone Derivative. *Int. J. Mol. Sci*. **2023**, 24, 5286.
7. Kedia, N.; Sarkar, A.; Shannigrahi, M.; Bagchi S. Photophysics of representative ketocyanine dyes: Dependence on molecular structure. *Spectrochim. Acta A* **2011**, 81, 79– 84.
8. Kessler, M.A.; Wolfbeis, O.S. *Spectrochim. Acta A* **1991**, 47A, 187-192
9. Vatsadze, S.Z.; Gromov, S.P. Novel Linear Bis-Crown Receptors with Cross-Conjugated and Conjugated Central Cores. *Macroheterocycles* **2017**, 10, 432–445.
10. Fomina, M.V.; Kurchavov, N.A.; Freidzon, A.Y.; Nuriev, V.N.; Vedernikov, A.I.; Strelenko, Y.A.; Gromov, S.P. Self-assembly involving hydrogen bonds. Spectral properties and structure of supramolecular complexes of bis-aza-18-crown-6-containing dienones with alkanediammonium salts. *J. Photochem. Photobiol. A* **2020**, 402, 112801.
11. Volchkov, V.V.; Khimich, M.N.; Melnikov, M.Y.; Egorov, A.E.; Starostin, R.O.; Freidzon, A.Ya.; Dmitrieva, S.N.; Gromov S.P. Hydrogen-Bonded Self-assembly of Supramolecular Donor–Acceptor Complexes of (E)-Bis(18-crown-6)azobenzene with Bis(ammoniopropyl) Derivatives of Bipyridine and Dipyridylethylene in Acetonitrile. *J. Solution Chem*. **2023**, https://doi.org/10.1007/s10953-023-01271-6.
12. Zou, Q.; Zhao, Y.; Makarov, N.S.; Campo, J.; Yuan, H.; Fang, D.C.; Perry, J.W.; Wu, F. Effect of alicyclic ring size on the photophysical and photochemical properties of bis(arylidene)cycloalkanone compounds. *Phys. Chem. Chem. Phys*., **2012**, 14, 11743–11752
13. Zou, Q.; Zhao, H.; Zhao, Y.; Wang, Y.; Gu, Y.; Wu, F. Polyethylene glycol-functionalized bis(arylidene)cycloalkanone photosensitizers for two-photon excited photodynamic therapy. *Proc. SPIE* **2012**, 8553, Optics in Health Care and Biomedical Optics V, 85530J
14. Dumur, F. Recent advances on benzylidene cyclopentanones as visible light photoinitiators of polymerization. *Eur. Polym. J*. **2022**, 181, 111639.
15. Sajan, D.; Lakshmi, K.U.; Erdogdu, Y.; Joe, I.H. Molecular structure and vibrational spectra of 2,6-bis(benzylidene)cyclohexanone: A density functional theoretical study. *Spectrochim. Acta A* **2011**, 78. 113–121
16. Gutrov, V.N.; Zakharova, G.V.; Fomina, M.V.; Gromov, S.P.; Chibisov, A.K. Intermediates of the Photoinduced 2,4-Bis(4-Diethylaminobenzylidene)cyclobutanone Redox Reaction in Methanol. *High Energy Chemistry*, **2020**, 54, 6, 436–440.
17. Zakharova, G.V.; Zyuz'kevich, F.S.; Nuriev, V.N.; Vatsadze, S.Z.; Plotnikov, V.G.; Gromov, S.P.; Chibisov, A.K. Photonics of Bis(diethylaminobenzylidene)cyclopentanone and Its Analogue with the Bisazacrown Moiety in Acetonitrile. *High Energy Chemistry*, **2016**, 50, 1, 27–31.
18. Zakharova, G.V.; Zyuz'kevich, F.S.; Gutrov, V.N., Gavrilova G.V., Nuriev, V.N.; Vatsadze, S.Z.; Plotnikov, V.G.; Gromov, S.P.; Chibisov, A.K. Effect of Substituents on Spectral, Luminescent and Time-Resolved Char-acteristics of 2,5-Diarylidene Derivatives of Cyclopentanone. High Energy Chemistry 2017, 51, 2, 113-117.
19. Zakharova, G.V.; Gutrov, V.N.; Nuriev, V.N.; Zyuz'kevich, F.S.; Vatsadze, S.Z.; Gromov, S.P.; Chibisov, A.K. Effect of Substituents on Spectral, Luminescent, and Time-Resolved Spectral Properties of 2,6-Diarylidene De-rivatives of Cyclohexanone High Energy Chemistry 2017, 51, 6, 424-426.
20. L.A. Huck, W.J. Leigh. A Better Sunscreen: Structural Effects on Spectral Properties. *Journal of Chemical Education*. **2010**, 87, 1384-1387.
21. Granovsky, A.A. Firefly Version 8.2.0. Available online: http://classic.chem.msu.su/gran/firefly/index.html (accessed on 28 October 2022).
22. Schmidt, M.W.; Baldridge, K.K.; Boatz, J.A.; Elbert, S.T.; Gordon, M.S.; Jensen, J.J.; Koseki, S.; Matsunaga, N.; Nguyen, K.A.; Su, S.; et al. General atomic and molecular electronic structure system. *J. Comput. Chem*. **1993**, *14*, 1347–1363.
23. Tomasi, J.; Mennucci, B.; Cammi, R. Quantum Mechanical Continuum Solvation Models. *Chem. Rev*. **2005**, *105*, 2999–3094.
24. Freidzon, A.Y.; Safonov, A.A.; Bagaturyants, A.A.; Alfimov, M.V. Solvatofluorochromism and Twisted Intramolecular ChargeTransfer State of the Nile Red Dye. *Int. J. Quantum Chem*. **2012**, *112*, 3059–3067.
25. Quentin, C.; Gerasimaite, R.; Freidzon, A.; Atabekyan, L.S.; Lukinavi˘cius, G.; Belov, V.N.; Mitronova, G.Y. Direct Visualization of ˙ Amlodipine Intervention into Living Cells by Means of Fluorescence Microscopy. *Molecules* **2021**, *26*, 2997.

 doi:10.20944/preprints202307.1488.v1